Cool Stars, Stellar Systems, and the Sun, 9th Cambridge Workshop
ASP Conference Series, Vol. 109, 1996
Roberto Pallavicini and Andrea K. Dupree (eds.)

Chromospheric and Coronal Heating Mechanisms

P. Ulmschneider
Institut für Theoretische Astrophysik, Universität Heidelberg, Tiergartenstr. 15, D-69121 Heidelberg, Germany

Abstract. The physical processes which are thought to provide steady heating of chromospheres and coronae are discussed. They can be classified as hydrodynamic and magnetic mechanisms. The magnetic mechanisms can be further subdivided into mhd-wave (AC) mechanisms and magnetic field dissipation (DC) mechanisms. Due to the common generation source, a correlation between the different mechanisms is expected.

1. Introduction

As very recently an extensive review of the mechanisms of chromospheric and coronal heating has been published elsewhere (Narain & Ulmschneider (1995), henceforth called Paper II), which updates earlier work by Narain & Ulmschneider (1990, Paper I), the present work concentrates on the discussion of the basic physical processes involved. For the detailed literature of this wide and complex field, as well as for additional reviews of this topic, I refer to Papers I and II as well as to the references therein. Section 2 summarizes the mechanical energy generation, while Section 3 discusses the various dissipation processes.

It has to be realized that most likely all discussed heating mechanisms are at work in an outer stellar atmosphere, although with different efficiency. The problem is that, so far, detailed investigations based on a realistic local physical state are largely missing, and thus a true assessment of the relative importance of the various mechanisms cannot be made. This situation is so bad even, that at the present time it can not be decided, whether AC or DC mechanisms are the dominant magnetic heating processes.

2. Mechanical Energy Generation

Table 1 gives a summary of the proposed mechanical heating mechanisms responsible for steady heating. Steady here means, that we do not discuss occasional localized events like large flares, but concentrate on the persistent processes, which provide a steady support of energy to balance the chromospheric and coronal losses. A heating mechanism consists of three processes, the *generation* of the mechanical energy carrier, the *energy transport* and the *energy dissipation.* Table 1 shows the various proposed energy carriers which can be classified as *hydrodynamic* and *magnetic* mechanisms, with the latter subdivided into wave or AC-mechanisms and DC-mechanisms.

Ultimately all mechanical energy carriers derive their energy from the nuclear processes in the stellar core. In late-type stars, this energy is transported in the form of radiation and convection to the stellar surface, where in the surface convection zone the generation of mechanical energy takes place. The mechanical energy generation results from the gas motions of the convection zone, which are largest in the regions of smallest density near the top boundary of that zone. Because of this the mechanical energy carriers, particularly the waves, are generated in a narrow surface layer.

Table 1. Mechanical heating mechanisms for stellar chromospheres and coronae, P is the wave period and P_A the acoustic cut-off period.

energy carrier	*dissipation mechanism*
hydrodynamic heating mechanisms	
acoustic waves, $P<P_A$	shock dissipation
pulsational waves, $P>P_A$	shock dissipation
magnetic heating mechanisms	
1. alternating current (AC) or wave mechanisms	
slow mode mhd waves, longitudinal mhd tube waves	shock dissipation
fast mode mhd waves	Landau damping
Alfvén waves (transverse, torsional)	mode-coupling resonance heating compressional viscous heating turbulent heating Landau damping
magnetoacoustic surface waves	mode-coupling phase-mixing resonant absorption
2. direct current (DC) mechanisms	
current sheets	reconnection (turbulent heating, wave heating)

As the gas motions in the convection zone can be described by a common temporal and spatial turbulence spectrum, consisting of a characteristic distribution from large to small gas bubbles and from long to short time scales, it is clear that different parts of that spectrum are correlated with one another. We thus expect to see correlations between the various heating mechanisms because of this common energy source.

2.1. Hydrodynamic Energy Generation

While in terrestrial situations monopole, dipole and quadrupole sound generation is a sequence of progressively less important ways to produce *acoustic waves*, this sequence is reversed in stellar situations, where external mass injections and rigid surfaces are absent. Here quadrupole sound generation is largest and, except for late-type dwarf stars, even dominant. Quadrupole sound generation from turbulence was originally developed by Lighthill and further extended by

Stein (1967) to stellar convection zones. The Lighthill-Stein theory was recently revisited by Musielak et al. (1994) and Ulmschneider, Theurer & Musielak (1996) who, using realistic turbulent energy spectra, computed acoustic fluxes and spectra for a large number of late-type stars with gravities of log g=0 to 8.

For quadrupole sound generation one starts from the linearized hydrodynamic equations, where one retains the small second order Reynolds stress term as source

$$\frac{\partial \rho'}{\partial t} + \nabla \cdot \rho_o \mathbf{v} = 0; \quad \rho_o \frac{\partial \mathbf{v}}{\partial t} + c_o^2 \nabla \rho' = -\nabla \cdot \rho_o \mathbf{vv}. \tag{1}$$

Here ρ_o is the density, $\mathbf{v}$ the velocity and c_o the sound speed. Operating with $\partial/\partial t$ on the first and $-\nabla\cdot$ on the second Eq. and adding, a wave equation with a source term can be derived

$$\left(\frac{\partial^2}{\partial t^2} - c_o^2 \nabla^2\right) \rho' = \nabla\nabla : \rho_o \mathbf{vv}. \tag{2}$$

As in a convection zone the convective velocities u are much smaller than c_o we replace in the source term $\mathbf{v} \rightarrow u$, $\nabla \rightarrow (u/c_o)\nabla' \sim (u/c_o^2)\partial/\partial t$. With this, Eq. (2) can be solved to give $\rho' \approx \rho_o u^4/c_o^4$. From the usual formula for the acoustic flux one then has

$$F_A = \frac{c_o^3 \rho'^2}{\rho_o} \approx \rho_o \frac{u^8}{c_o^5} \approx \int_{\Delta z} 38 \rho_o \frac{u^8 dz}{c_o^5 H}, \tag{3}$$

which is the famous Lighthill-Proudman formula where a Kolmogorov type turbulent energy spectrum was used. Here z is height and H the pressure scale height. In terrestrial applications (jet noise) excellent agreement of the u^8-dependence with observations has been found, see Paper II.

The *pulsational waves*, most prominent in Mira-type stellar pulsations, but also in other late-type giants, is generated by the kappa-mechanism. The kappa-mechanism functions similarly as the internal combustion engine in motorcars. In the internal combustion engine a reactive gas mixture is compressed in a pulsational motion and is ignited at the moment of strongest compression resulting in a violent decompression. This ensures that the pulsational motion is amplified. In the kappa-mechanism the opacity of stellar envelope material increases (due to the adiabatic temperature and pressure increase), when the star contracts in a pulsational motion. This opacity increase leads to an increased absorption of radiation and thus to a large heat input into these envelope layers. The overheated envelope layers subsequently react by rapid expansion, thus driving the pulsation. These pulsational waves propagate to the outer stellar atmosphere where they form shocks.

This same process, in principle and possibly with different drivers, works also for nonradial oscillations. Any process which kicks on the basic pulsational and vibrational modes of the outer stellar envelope belongs to the category pulsational wave mechanism. For the Sun the 3 min oscillation is such an example of a basic resonance which is generated by transient events produced by the convection zone. A systematic study of this heating mechanism for late-type stars is missing at the present time.

2.2. Magnetic Energy Generation

Consider a cylindrical magnetic flux tube of length $l_{||}$ and diameter $l_{\perp}$ where the magnetic field B is along the axis of the tube. The convective gas motions outside the tube lead to magnetic field perturbations δB either in tangential or in radial direction. One then has $\delta B \approx B l_{\perp}/l_{||} \approx B u \tau / l_{||}$, where u is the velocity and τ the characteristic time of the convective flow. From this the energy density of the perturbation is (where c_A is the Alfvén speed)

$$E = \frac{\delta B^2}{4\pi} \approx \frac{B^2}{4\pi}\left(\frac{u}{l_{||}}\right)^2 \tau^2 = \rho_o c_A^2 \left(\frac{u}{l_{||}}\right)^2 \tau^2 \,. \tag{4}$$

1. For slow tube motion ($\tau > l_{||}/c_A$) one has a generated energy flux for the DC-mechanism

$$F_{DC} = E\frac{l_{||}}{\tau} = \rho_o c_A^2 \frac{u^2}{l_{||}}\tau, \tag{5}$$

2. for fast tube motion ($\tau < l_{||}/c_A$), with an effective $l_{||} = c_A \tau$, one has a generated energy flux for the AC-mechanism

$$F_{AC} = \rho_o u^2 c_A. \tag{6}$$

In order to derive numerical values for these fluxes one must obtain convective velocities theoretically or by observation. For the computation of transverse and longitudinal wave fluxes, based on realistic estimates of the turbulent energy spectrum, both analytical and numerical procedures were recently developed. The analytical approach derives the fluxes similar as in the Lighthill-Stein theory. The numerical approach works by directly exciting magnetic flux tubes. For details and literature references see Paper II.

From the derivation of the above fluxes it is again obvious that they result from one global turbulent energy spectrum and thus are expected to be partly correlated. Clearly, slow flows involved in the formation of current sheets, when sunspot groups approach one another, or when magnetic arcade fields are sheared, are only very loosely correlated with the rapid local flows which generate waves. There is presently no theory to compute torsional wave fluxes.

3. Energy Dissipation

3.1. The dissipation process

In the dissipation process, mechanical energy is converted into heat. That is, organized motion or potential energy is converted into random thermal motion. As will be shown below, an efficient conversion process is almost always associated with the formation of large variations of the physical variables over very small scales. For instance, it has been known for a long time that an efficient way to dissipate acoustic waves is the formation of shocks, where the physical variables jump over distances of a molecular mean free path. Thus in recent years considerable effort has gone into the study of how, in magnetic field regions, areas with small scales develop naturally (Papers I and II).

Consider a typical mhd wave in the solar chromosphere with characteristic parameters, half wavelength $L = 200\ km$, temperature $\Delta T = 1000\ K$, velocity $\Delta v = 3\ km/s$ and magnetic field perturbation $\Delta B = 10\ G$. Using appropriate values for the thermal conductivity $\kappa = 10^5\ erg/cm\ s\ K$, viscosity $\eta = 5 \cdot 10^{-4}\ erg\ s/cm^3$ and electrical conductivity $\lambda_{el} = 2 \cdot 10^{10}\ s^{-1}$ we find for *the thermal conductive heating rate:*

$$\Phi_C = \frac{d}{dz}\kappa\frac{dT}{dz} \approx \frac{\kappa\Delta T}{L^2} \approx 3 \cdot 10^{-7} \quad \left[\frac{erg}{cm^3 s}\right] \tag{7}$$

the viscous heating rate:

$$\Phi_V = \eta\left(\frac{dv}{dz}\right)^2 \approx \frac{\eta\Delta v^2}{L^2} \approx 1 \cdot 10^{-7} \quad \left[\frac{erg}{cm^3 s}\right] \tag{8}$$

the Joule heating rate:

$$\Phi_J = \frac{J^2}{\lambda_{el}} = \frac{c_L^2}{16\pi^2\lambda_{el}}(\nabla \times B)^2 \approx \frac{c_L^2\Delta B^2}{16\pi^2\lambda_{el}L^2} \approx 7 \cdot 10^{-5} \quad \left[\frac{erg}{cm^3 s}\right]. \tag{9}$$

Here J is the current density and c_L the light velocity. The three heating rates show that normally these processes are inadequate to balance the empirical chromospheric cooling rate of $10^{-1} erg/cm^3\ s$. Only when the length scale L is considerably decreased, can the heating rates be raised to acceptable levels. For acoustic waves as well as slow mode mhd- and longitudinal mhd tube waves, this is accomplished by shock formation. For magnetic cases, by the formation of current sheets.

3.2. Mode-coupling

This mechanism is not a heating process by itself, but converts wave modes, which are difficult to dissipate, by non-linear coupling into other modes, where the dissipation is more readily achieved. Typical cases are the conversion of transverse or torsional Alfvén waves into acoustic-like longitudinal tube waves. For examples of these two processes see Papers I and II.

3.3. Resonance heating

Resonance heating occurs, when upon reflection of Alfvén waves at the two foot points of the coronal loops, one has constructive interference. For a given loop length $l_{||}$ and Alfvén speed c_A, resonance occurs, when the wave period is $mP = 2l_{||}/c_A$, m being a positive integer. Waves which fulfill the resonance condition are trapped and after many reflections are dissipated by Joule-, thermal conductive or viscous heating. Examples of this process are given in Papers I and II.

3.4. Compressional viscous heating

Compressional viscous heating, recently proposed by Strauss (1991, see also Paper II), is a very promising mechanism for coronal regions, where the gyro frequency is much larger than the collision frequency. Swaying an axial magnetic

flux tube sideways with velocity $\mathbf{v}_\perp$ results in a transverse Alfvén wave which is incompressible ($\nabla \cdot \mathbf{v}_\perp = 0$) to first order. This is different for tubes with helicity, where one has $\nabla \cdot \mathbf{v}_\perp \approx \dot{\rho}/\rho$. With an increase of the density, the magnetic field is compressed and the gyro frequency increased. Gyrating around the field lines more quickly, the ions after colliding with each other, generate larger velocities in non-perpendicular directions as well, which constitutes the heating process.

3.5. Turbulent heating

In a turbulent flow field with high Reynolds number there are bubbles of all sizes. The energy usually is put into the largest bubbles. Because of the large inertial forces the big bubbles are ripped apart into smaller bubbles, and these in turn into still smaller ones etc. This process is called turbulent cascade. A turbulent flow field can be described by three characteristic quantities, density ρ_o, bubble scale $l_k = 2\pi/k$, and the mean velocity u_k of such bubbles. k is the wavenumber. It is easily seen, that from these three quantities only one combination for a heating rate can be formed:

$$\Phi_k = \rho_o \frac{u_k^3}{l_k} \quad \left[\frac{erg}{cm^3 s}\right]. \tag{10}$$

If there are no other losses, like by radiation, all the energy which is put in at the largest bubbles must reappear in the smaller bubbles etc. Thus if $k1, k2, \cdots$ represents a series of smaller and smaller bubbles one must have $\Phi_{k1} = \Phi_{k2} = \cdots = \text{const}$. This implies

$$u_k \sim l_k^{1/3}, \tag{11}$$

which is the *Kolmogorov law*. The range $l_{k1} \cdots l_{kn}$ of validity of this law is called the *inertial range*. Consider what happens if l_k becomes very small. From Eqs. (8) and (11) one finds for the viscous heating rate $\Phi_V = \eta(du/dl)^2 \approx \eta u_k^2/l_k^2 \approx \eta l_k^{-4/3}$, which goes to infinity for $l_k \to 0$. Thus at some small enough scale, viscous heating sets in and the inertial range ends. It is seen that turbulent heating lives from the formation of small scales. One can visualize the process as follows. Because of the continuous splitting of bubbles into smaller sizes, with the velocities decreasing much less rapidly, one eventually has close encounters of very small bubbles with large velocity differences where viscous heating dominates. For recent work on turbulent heating see Papers I and II.

3.6. Landau damping

Landau damping occurs at coronal heights, where the collision rate becomes small. As Chen (1984, Fig. 7.17) has well explained, this process is analogous to surfing on ocean waves. When surfing, a surfboard rider launches himself in propagation direction into the steepening part of an incoming wave and gets further accelerated by this wave. In Landau damping, the propagating wave accelerates gas particles which, due to their particle distribution function, happen to have similar direction and speed as the wave. Because a distribution function normally has many more slower particles than faster ones, the wave looses energy to accelerate the slower particles. This gained energy is eventually shared with other particles in the process to reestablish the distribution function (see Papers I and II), which constitutes the heating mechanism.

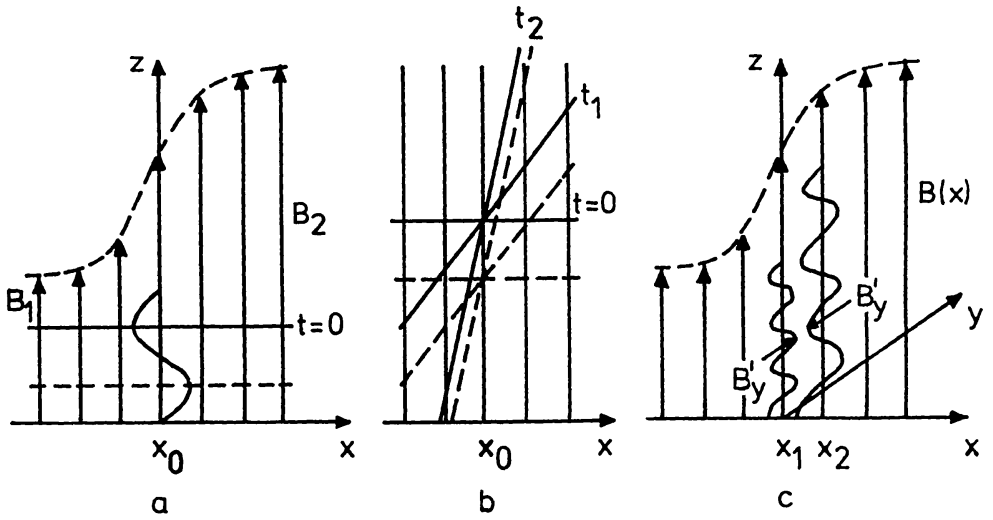

Figure 1. In a field pointing in z-direction, where the field strength varies in x-direction: a) resonant absorption of a surface wave (shaking in x-direction), wave fronts at time $t = 0$, b) these wave fronts at subsequently later times t_1, and t_2, c) phase-mixing of a surface wave (shaking in y-direction).

3.7. Resonant absorption

In the process of resonant absorption one considers magnetoacoustic surface waves in a magnetic field B which points in z-direction, and varies from B_1 to B_2 in x-direction (see Figure 1). The surface wave, with its field perturbation $\delta B = B'_x$ in x-direction, has a phase speed $v_{ph} = ((B_1^2 + B_2^2)/(4\pi(\rho_1 + \rho_2))^{1/2}$, such that at an intermediate position x_o, the phase speed becomes equal to the local Alfvén speed $c_{Ao} = B(x_o)/\sqrt{4\pi\rho(x_o)}$. In panel a of Figure 1 consider the wave fronts of the peak (drawn) and trough (dotted) of a surface wave. Because to the right of x_o, the Alfvén speed is larger and to the left smaller, the wave fronts at a later time get tilted, relative to the phase, propagating with speed c_{Ao} (see panel b). At a still later time (panel b) the wave fronts get tilted even further and approach each other closely at the position x_o. This leads to small scales and intense heating at that field line. For the recent extensive analytical and numerical work on this heating process see Papers I and II as well as the references therein.

3.8. Phase-mixing

For phase-mixing (c.f. panel c of Figure 1) one considers the same magnetic field geometry as in panel a of Figure 1, however, the field perturbation $\delta B = B'_y$ of the wave is now in y-direction, perpendicular to the x- and z-directions. As the Alfvén speeds of two closely adjacent regions x_1 and x_2 in x-direction are different, it is seen that after propagating some distance Δz, the fields $B'_y(x_1)$ and $B'_y(x_2)$ will be very different, leading to a current sheet and strong dissipation. Here again it is the appearance of small scale structures which lead to dissipation (see Papers I and II).

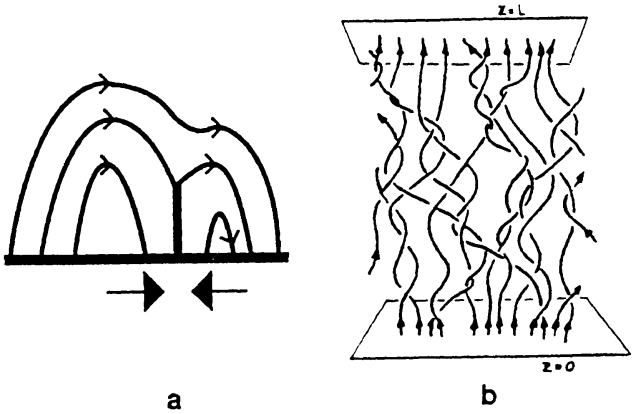

Figure 2. Current sheets in arcades (left) and at various places in tangled fields (right).

3.9. Reconnection

As examples of the DC heating mechanisms, Figure 2 shows two different situations where current sheets are thought to exist. The left panel, after Priest (1991), shows an arcade system, which by slow motion is laterally compressed and develops a current sheet, where oppositely directed fields reconnect. The right panel, after Parker (1992), displays a tangled and braided web of coronal loops created by slow foot point motions. The loops are drawn in such a way that the two foot points, where the tangling motion occurs, are at the top and bottom. Energized by the convection zone, the system tries to return to its minimum energy configuration. This can only be done by reconnection. At many locations in the web oppositely directed fields occur, giving rise to local current sheets, which by reconnection (in the form of microflares) release the magnetic field energy. The energy is dissipated both directly and via the generation of waves and turbulence. Note that reconnection likewise happens in small scale regions. For recent work on current sheets and microflare heating see Papers I and II.

References

Chen, F.F. 1984, Introduction to Plasma Physics and Controlled Fusion 2^{ed}, Vol 1, Plasma Physics, Plenum Press, New York

Narain, U., Ulmschneider, P. 1990, Space Sci.Rev., 54, 377 (Paper I)

Narain, U., Ulmschneider, P. 1995, Space Sci.Rev., in press (Paper II)

Musielak Z.E., Rosner R., Stein, R.F., Ulmschneider P. 1994, ApJ, 423, 474

Parker, E.N. 1992, J. Geophys. Res. 97, 4311

Priest, E.R. 1991, in Mechanisms of Chromospheric and Coronal Heating, Eds. Ulmschneider P., Priest E.R., Rosner R., Springer, Berlin, p 520

Stein, R.F. 1967, Solar Phys., 2, 385

Strauss, H.R. 1991, Geophys. Res. Let., 18, 77

Ulmschneider, P., Theurer, J., Musielak, Z. 1996, A&A, submitted